Driving Sudden Current and Voltage in Expanding and Compressing Plasma

P. F. Schmit and N. J. Fisch

Department of Astrophysical Sciences, Princeton University, Princeton, New Jersey 08544, USA

(Received 16 January 2012; revised manuscript received 13 March 2012; published 23 May 2012)

A magnetized plasma preseeded with an initially undamped Langmuir wave is shown to transition suddenly to a collisionless damping regime upon expansion of the plasma perpendicular to the background magnetic field. The resulting anisotropic fast-particle distribution then leads to an electrical current and dc voltage induction. The current drive efficiency of this effect in nonstationary plasmas is shown to depend on the rate of expansion of the plasma, the time-varying collisionality, and the plasma L/R time. Subsequent recompression of the plasma enhances this current drive effect by reducing further the collision rate of the current-carrying electrons.

DOI: 10.1103/PhysRevLett.108.215003 PACS numbers: 52.35.Fp, 47.10.ab, 52.25.−b, 52.65.Rr

Introduction.—Time-varying plasma with embedded waves [1] or dust [2] can often exhibit radically different behavior from steady state plasma. Here, a new scheme to drive sudden bursts of current and voltage is predicted in nonstationary plasma, whereby an initially undamped monochromatic wave, embedded in a magnetized plasma and propagating in one direction parallel to the magnetic field, is induced into wave-particle resonance with plasma particles due to magnetic expansion perpendicular to the wave vector. The sudden, collisionless damping causes the wave to transfer its energy anisotropically onto the comoving high-energy tail of the resonant particle distribution, while subsequent velocity-dependent collisional relaxation of the modified distribution results in a rise and fall of the total fast-particle current.

As a paradigmatic example, embedded Langmuir waves are considered, though other waves may prove more suitable for specific applications. The peak attainable fast-particle current densities occur for expansion rates, η, comparable to the electron collision rate, ν_c. However, expansion rates significantly faster than the collision rate lead to more prolonged current as a result of enhanced electron trapping by the wave, which carries more electrons to superthermal velocities and, hence, reduces their collisionality. Interestingly, the current can be prolonged by magnetically compressing the plasma to higher densities following the collisionless damping, which increases perpendicular velocities sufficiently to lower the collisionality of the current-carrying electrons.

Before presenting the results of the numerical simulations, the basic current drive mechanism will be explained briefly. For slow variation of external forces, the Langmuir wave dispersion relation obeys the eikonal equation [3]: $\omega^2 = \omega_p^2(t) + 3k^2 v_{T\|}^2(t)$, where ω_p is the plasma frequency, and $v_{T\|}$ is the electron thermal velocity in the direction parallel to the wave vector $\mathbf{k}$, with $|\mathbf{k}| \equiv k$. This is just the normal dispersion relation for plasma oscillations, but with ω_p and $v_{T\|}$ varying slowly in time. Assume there exists a homogeneous magnetic field $\mathbf{B} \parallel \mathbf{k}$ that is sufficiently strong to magnetize both the ions and the electrons. Then, the plasma number density $n \propto |\mathbf{B}| \equiv B(t)$ by magnetic flux freezing, as B is slowly varied with time. Additionally, the conservation of the magnetic moment, $\mu = m v_\perp^2/2B$, on time scales short compared to ν_c^{-1} leads to the reduction of perpendicular velocities for magnetic expansion, i.e., $dB/dt < 0$.

Consider, for simplicity, a torus of plasma in a toroidal magnetic field. The torus is high aspect ratio, so any small toroidal segment appears cylindrical, and expansion is presumed to occur in the minor radius only, while the major radius is fixed. Initially, the phase velocity of an embedded Langmuir wave $v_{ph} = \omega/k \gg v_{T\|}$, with $k =$ const, and $\omega \approx \omega_p \propto n^{1/2}$ for perpendicular expansion. Neglecting anisotropy-driven electromagnetic instabilities (addressed in the *Discussion* section), $v_{T\|}$ is decoupled from $v_{T\perp}$ when $\nu_c \ll \eta$, and the wave can be made to satisfy the condition $v_{ph} \sim \mathcal{O}(v_{T\|})$ via magnetic expansion, at which point Landau damping of the wave initiates [1]. Even in the limit $\nu_c \sim \mathcal{O}(\eta)$, where the temperature variation scales with the system volume adiabatically, i.e., $TV^{2/3} =$ const, one still finds $v_T \propto n^{1/3}$. Thus, in this limit the ratio $v_{ph}/v_{T\|} \propto n^{1/6}$, and the Landau damping criterion still can become satisfied.

As opposed to the case of compression parallel to $\mathbf{k}$ by walls, where only heating occurs [1], here the Landau damping of a wave traveling in one direction forms an anisotropic high-energy electron tail. For an electrostatic plasma wave initially far from resonance, the fields carry no momentum ($\mathbf{E} \times \mathbf{B} = 0$), while the velocity perturbation to the thermal electrons in response to the wave is sinusoidal, so net mechanical momentum also averages to zero. Nonlinear Landau damping is expected to conserve total momentum; thus, velocity-dependent collisions between electrons and ions are needed in order for an electric current to arise [4]. Since particle collision rates $\nu_c \sim 1/v^3$, the high velocity tail relaxes more slowly than the rest of the distribution, producing a net current. However,

as opposed to steady state current drive [5], here the development and relaxation of current carried by suprathermal particles will be impacted significantly by the time-varying temperature and density of the plasma as well as inductive effects [6].

Induced wave damping in expanding plasma.—To describe this *switchlike* mechanism, a novel particle-in-cell (PIC) simulation was developed that treats electrostatic fields with mobile electrons and ions in one spatial dimension, while particle velocities parallel and perpendicular to the simulation domain are modeled. Periodic boundary conditions are imposed to allow the current loop to close, and the velocities are initialized as Maxwellian with a sinusoidal parallel perturbation for the plasma wave. Perpendicular velocities are coupled to the change in n (and thus $\mathbf{B}$) by enforcing conservation of the magnetic moment, $\Delta\mu = 0$, during each time step, $\Delta t \ll \omega_p^{-1} \ll \nu_c^{-1}$. Variations in density due to perpendicular compression and expansion are simulated by scaling both the PIC particle charge, Q, and mass, M, proportionally to the normalized density, $\tilde{n}_j = n_j/n_0$, while holding the ratio Q/M fixed. This can be visualized as the redistribution of charge across the perpendicularly homogeneous charge sheets modeled by a 1D PIC code. Finally, a continuous, time-explicit PIC collision algorithm for coupling parallel and perpendicular velocities was used based on the approach in Ref. [7]. The advantage of this approach is that the 2D effects of magnetic expansion and collisional relaxation can be retained while simulating motion in only one spatial dimension, allowing for more particles to be simulated per cell, and, hence, drastically decreasing the statistical noise.

Any time-varying current will induce an electric field, whose strength will depend on the L/R time, τ. The total current then can be described by [8]: $\tau dI/dt = I_{\mathrm{rf}}(t) - I$, where $I_{\mathrm{rf}}(t)$ is the current source that arises from the effects considered here. Since the number of fast current carriers is small compared to the bulk current carriers, the induced electric field affects primarily bulk electrons, producing current with classical resistivity. What is addressed and simulated here is the wave-generated current, $I_{\mathrm{rf}}(t)$, for which the induced field can be ignored [6]. Thus, a different choice of plasma parameters and expansion rate could yield a switchlike means to produce either a burst of current or voltage, or both.

Consider a Langmuir wave that is initialized such that the trapping width $v_{\mathrm{tr}}/v_{\mathrm{T}} = 3$, and the phase velocity $v_{\mathrm{ph}}/v_{\mathrm{T}} = 7$, where $v_{\mathrm{tr}} = 2\sqrt{eE/mk}$, E is the electric field strength, and e/m is the electron charge-to-mass ratio. Particles are not initialized beyond $v_{\parallel} = 4v_{\mathrm{T}}$ in velocity-space, so the resonant region of the wave initially lies just beyond the fastest particles in the simulation, and no damping occurs if collisions are excluded and the density is held fixed. The plasma density is chosen so the electron collisionality relative to the wave frequency ω initially goes

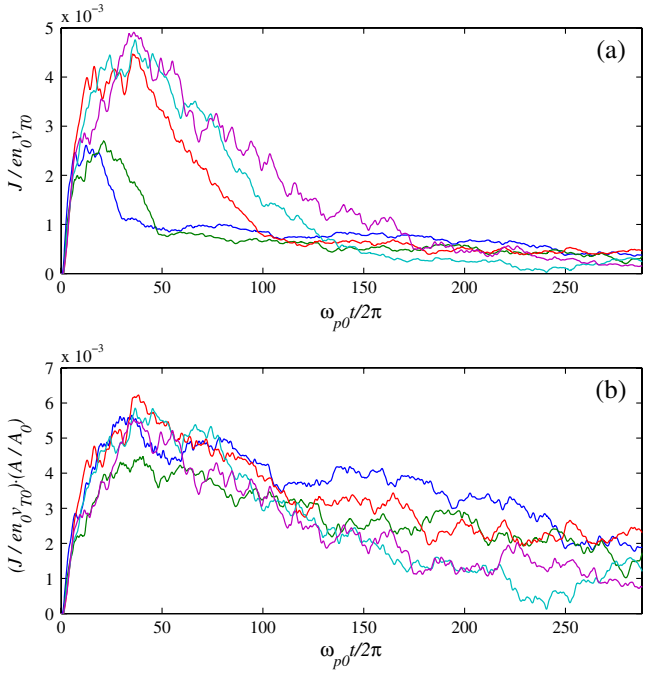

FIG. 1 (color online). (a) Dimensionless current density for expansion time $\mathcal{T} = 30$ (blue), 50 (green), 100 (red), 150 (cyan), 250 (magenta), time measured in units τ_{p0}. (b) Dimensionless total flux tube current, same color scheme.

like $\omega/2\pi\nu_c = 94$, and an optimal expansion rate, η, is expected to exist in the range $\omega \gg \eta \gtrsim \nu_c$, where sufficient collisionless damping can occur before the wave energy is lost to collisional damping. The plasma is expanded until it is 20% of its original density at different linear rates with brief, smooth ramp-up and ramp-down periods. Following expansion, the plasma is allowed to evolve further at the fixed reduced density.

The fast-particle current response of the plasma subject to a number of different expansion times, $\mathcal{T} = 1/\eta$, is shown in Fig. 1. Figure 1(a) shows the normalized current density, J/en_0v_{T0}, versus time for $\mathcal{T} = 30$, 50, 100, 150, and 250, where $\mathcal{T}$ has units of plasma periods, $\tau_{p0} = 2\pi/\omega_{p0}$, and the subscript "0" signifies an initial value. Since the PIC code utilizes a random collision routine, the data in Fig. 1 represent the mean of many identically initialized simulations for each value of $\mathcal{T}$, with an ω_p-scale smoothing filter applied to remove fast oscillations. The statistical error in the data is on the order of $\pm 1 \times 10^{-4}$ for Fig. 1(a), approximately a 2% to 5% error at peak current density. To maximize the peak current density, there is clearly a benefit to slower expansion, though the performance levels off for $\mathcal{T} \gtrsim \mathcal{O}(\nu_c^{-1})$. Of course, for $\mathcal{T} \gg \nu_c^{-1}$, the wave damps promptly without modifying the tail distribution significantly.

Figure 1(b) shows the total normalized flux tube current. The peak current is far less sensitive to $\mathcal{T}$ than the peak current density, though Fig. 1(b) shows that *faster* expansion

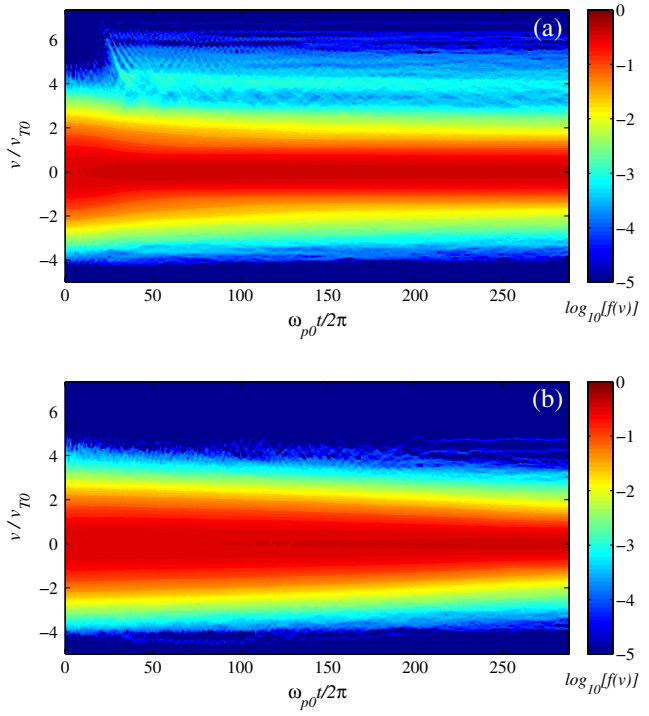

FIG. 2 (color online). Plot of $\log_{10}[f(v,t)]$, with $f(v,t)$ the electron parallel velocity distribution function, for (a) $\mathcal{T} = 30\tau_p$ and (b) $\mathcal{T} = 250\tau_p$. Cooling of bulk parallel velocities is due to collisional coupling with perpendicular velocities.

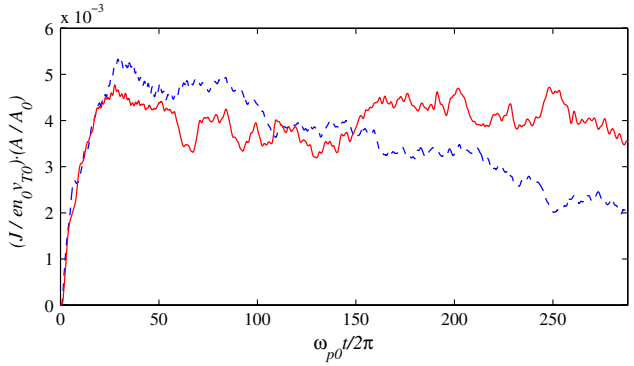

FIG. 3 (color online). Normalized flux tube current for the original $\mathcal{T} = 30\tau_p$ expansion scenario (dashed line), and where the plasma is compressed immediately back to its original density with an identical ($\mathcal{T} = 30\tau_p$) linear profile (solid line).

generally leads to a more prolonged current profile. Thus, another figure of merit might be the total time-integrated current. In this case, optimization of time-integrated current also points to faster expansion rates. Figure 2(a) shows the behavior of the normalized electron parallel velocity distribution function, $f(v)$, with $\int f(v)dv = 1$, for $\mathcal{T} = 30\tau_{p0}$. At this expansion rate, enhanced particle trapping by the wave modifies significantly the particle distribution in the vicinity of the resonance [9], accelerating high-energy electrons to higher parallel velocities by amounts comparable to $v_{\rm tr}$. On the other hand, Fig. 2(b) shows that slower expansion leads to less particle trapping, thus limiting the production of high-energy electrons. In phase space, the advancement of the trapped orbit separatrix along the velocity axis toward the particle distribution, i.e., $d/dt|v_{\rm ph}/v_{\rm T\|}| \equiv \alpha < 0$, is counterbalanced by the recession of the separatrix due to wave damping, i.e., $d/dt(v_{\rm tr}/v_{\rm T\|}) \equiv \gamma < 0$. This reduction in $v_{\rm tr}$ is due initially to plasmon conservation as the plasma rarefies, $v_{\rm tr} \propto E^{1/2} \propto n^{3/8}$ [3], and later to resonant wave-particle energy exchange, $\dot{v}_{\rm tr} \approx \gamma_{\rm L} v_{\rm tr}/2$, with the (nonlinear) Landau damping coefficient, $\gamma_{\rm L} \lesssim 0$ [9]. Then, when $|\alpha| \gg |\gamma|$, as is the case with fast system expansion, a phase space bubble is dragged into the plasma, and resonant particles experience an impulse of $\mathcal{O}(v_{\rm tr})$ [10]. As some particles become trapped by the wave, an additional downshift in wave frequency occurs [11], dragging the phase space bubble further into the thermal velocity distribution. In the slower expansion case, where $|\alpha| \approx |\gamma|$, the wave damps appreciably as it penetrates the distribution, limiting the size of the phase space bubble. Consequently, the current carriers in the slower expansion cases are significantly lower energy relative to the high-energy current carriers produced in the faster expansion cases, resulting in quicker collisional damping of the associated current.

Extended current with recompression.—The lifetime of the modified parallel velocity tail can be extended significantly through magnetic recompression of the plasma following collisionless damping of the wave. Figure 3 shows the flux tube current for the original $\mathcal{T} = 30\tau_{p0}$ case from Fig. 1(b) as well as the case where, after $t = \mathcal{T}$, the plasma is then compressed back to its original density at the same linear rate. The current in the recompressed plasma decays over a longer interval, since the compression heats the particles at a rate sufficient to overcome the opposing effect of densification, lowering the overall collisionality. Generally, simulations reveal that faster recompression leads to more prolonged current.

Discussion.—The use of lower dimensional models to simulate wave-particle interactions often offers benefits and has been implemented recently in other systems [12]. The number of particles N_S required in an S-dimensional PIC simulation is determined by the weak-coupling condition, $N_S(\lambda_{\rm D}/L)^S \gg 1$, where $\lambda_{\rm D}$ is the Debye length and L is the characteristic length of the simulation domain. Since $\lambda_{\rm D}/L \ll 1$, far fewer particles are needed in a one-dimensional simulation. The lower dimensionality of the code also allows N to be increased beyond the minimum requirements so that noise, scaling like $1/\sqrt{N}$, may be reduced without loss of computational tractability.

The simulation does not treat electromagnetic interactions and, thus, does not capture temperature anisotropy-driven instabilities [13]. For $a \equiv T_\perp/T_\|$, the relevant electron instabilities, the firehose ($a < 1$) and whistler ($a > 1$) instabilities, have maximum growth rates determined by

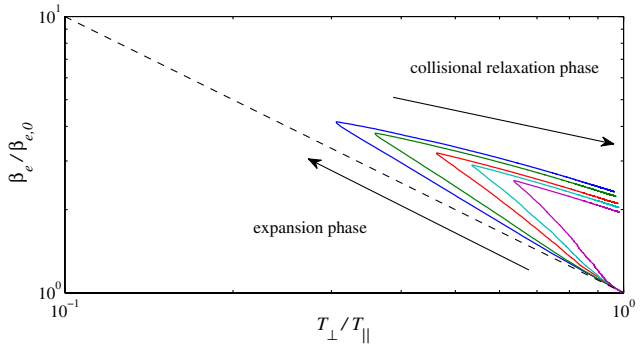

FIG. 4 (color online). Plot of system trajectories in $a - \beta_e$ space (parameters defined in text). Same color scheme as Fig. 1. Dashed line shows the reversible pathway for $\eta \gg \nu_c$.

two parameters: parallel beta, $\beta_e = 8\pi n T_\parallel / B^2$, and the anisotropy parameter, a. The systems modeled in Fig. 1 traverse this parameter space as indicated in Fig. 4. Initial conditions correspond to the lower right corner of the plot, and, given enough time, all trajectories eventually return to $a = 1$ from collisional isotropization. The dashed line shows the limit of $\eta \gg \nu_c$, in which $\beta_e \propto n^{-1}$, and $a \propto n$, so the (reversible) paths are along lines of constant $a\beta_e$. Figure 4 can be compared directly with Fig. 5 of Ref. [13(b)]. For expansion-induced current, which coincides with $a < 1$, the firehose instability generally can be avoided by picking a sufficiently small β_{e0}. On the other hand, the whistler instability, whose growth rate is more sensitive to anisotropy than the firehose instability, may occur with recompression if $a > 1$, limiting the extent to which plasma compression may prolong the current.

The simulation also does not capture the induced electric field due to finite $\dot{I}_{\rm rf}$. However, Appendix A of [6] shows that the relaxation of the fast-particle current is minimally affected by the induced dc field driving an Ohmic countercurrent. Then the $I_{\rm rf}(t)$ calculated here can be inserted into the circuit equation along with some L/R time [8], and the solution $I(t)$ then represents the net plasma current. Because there is a trade-off between driven current and induced voltage, a continuum of parameter-dependent plasma responses can be achieved through this switchlike wave damping mechanism.

The analysis here describes Langmuir waves propagating along field lines of a toroidally magnetized annulus of plasma expanding uniformly about its toroidal axis. Such a wave could be excited by external injection of an electron beam [14] or using chirped lasers [15], for example. In one scenario, a single current-carrying wire runs along the central axis of a Z-pinch, producing an azimuthal magnetic field within the plasma surrounding the wire. At temperatures near 750 eV and densities of $\mathcal{O}(10^{16}\ \mathrm{cm}^{-3})$, an $\mathcal{O}(100\ \mu\mathrm{m})$ Langmuir wave with energy density roughly 1% the total plasma energy would drive several $\mathrm{kA/cm}^2$ of fast-particle current with expansion times $\mathcal{T} \sim 100$ ns, characteristic of modern Z-pinch devices [16]. However, note that a toroidal plasma with major radius $\mathcal{R}$ and minor radius a exhibits resistance scaling like $R \sim \mathcal{R}\eta/a^2$, with the classical resistivity $\eta \sim 4\pi\nu_c/\omega_p^2$. The inductance scales like $L \sim 4\pi\mathcal{R}/c^2$, leading to the scaling $L/R \sim (a/\delta_e)^2/\nu_c$, with the electron skin depth $\delta_e = c/\omega_p$. For a cm-scale Z pinch with the above parameters, $\mathcal{T} \ll L/R$, and an $\mathcal{O}(1\ \mathrm{mV})$ loop voltage nearly cancels $I_{\rm rf}$. Instead, significant net current is produced when $L/R \lesssim \mathcal{T} \lesssim \nu_c^{-1}$, implying $a/\delta_e \lesssim 1$. For instance, centimeter waves in magnetically confined laboratory plasmas, with densities around $10^{10}\ \mathrm{cm}^{-3}$ and temperatures around 50 eV, produce current at sub-ms expansion times. Note, though, that so long as $L/R \lesssim \nu_c^{-1}$, fast-particle current driven by relatively fast expansion, i.e., $\mathcal{T} \ll L/R$, will eventually produce net current long after expansion has ceased, since $I_{\rm rf}$ decays on a much longer time scale than ν_c^{-1}.

While Langmuir waves serve as a paradigmatic example to illustrate the current drive mechanism, various applications may find other waves more suitable, such as lower frequency waves or nonlinear waves [17]. Waves characterized by coherent motion of the ion species would damp on ion collisional time scales, allowing for more modest expansion rates and/or higher initial plasma densities. Lower frequency waves also could be made to damp preferentially on the ions, in which case the formation of an enhanced superthermal ion population could be of practical use in inertial fusion experiments [18].

In summary, magnetic expansion of plasma can induce sudden collisionless damping of an embedded Langmuir wave with phase velocity in one direction. This produces a fast-particle current that grows and subsides due to a dynamically changing collision rate, while inductive effects drive a loop voltage and Ohmic countercurrent. The efficiency of this current drive process varies with the expansion rate of the plasma, with faster rates leading to longer-lasting currents due to greater particle trapping by the wave. This current drive effect is enhanced further by the subsequent recompression of the plasma.

This work was supported by the U.S. Defense Threat Reduction Agency, the DOE under Contract No. DE-AC02-09CH11466, and by the NNSA SSAA Program through DOE Research Grant No. DE-FG52-08NA28533.

[1] P. F. Schmit, I. Y. Dodin, and N. J. Fisch, Phys. Rev. Lett. **105**, 175003 (2010).
[2] K. Avinash, R. L. Merlino, and P. K. Shukla, Phys. Lett. A **375**, 2854 (2011).
[3] I. Y. Dodin, V. I. Geyko, and N. J. Fisch, Phys. Plasmas **16**, 112101 (2009).
[4] N. J. Fisch and A. H. Boozer, Phys. Rev. Lett. **45**, 720 (1980).
[5] N. J. Fisch, Phys. Rev. Lett. **41**, 873 (1978).
[6] P. F. Schmit and N. J. Fisch, Phys. Plasmas **18**, 102102 (2011).
[7] A. V. Bobylev and K. Nanbu, Phys. Rev. E **61**, 4576 (2000).

[8] N. J. Fisch, Rev. Mod. Phys. **59**, 175 (1987).
[9] T. O'Neil, Phys. Fluids **8**, 2255 (1965); G. Manfredi, Phys. Rev. Lett. **79**, 2815 (1997).
[10] L. Friedland, P. Khain, and A. G. Shagalov, Phys. Rev. Lett. **96**, 225001 (2006).
[11] I. Y. Dodin and N. J. Fisch, Phys. Plasmas **19**, 012103 (2012).
[12] J. W. S. Cook, S. C. Chapman, R. O. Dendy, and C. S. Brady, Plasma Phys. Controlled Fusion **53**, 065006 (2011).
[13] (a) S. P. Gary, M. D. Montgomery, W. C. Feldman, and D. W. Forslund, J. Geophys. Res. **81**, 1241 (1976); (b) S. P. Gary and C. D. Madland, J. Geophys. Res. **90**, 7607 (1985).
[14] B. Lefebvre, L. J. Chen, W. Gekelman, P. Kintner, J. Pickett, P. Pribyl, and S. Vincena, Nonlinear Proc. Geophys. **18**, 41 (2011).
[15] M. Deutsch, B. Meerson, and J. E. Golub, Phys. Fluids B **3**, 1773 (1991).
[16] S. L. Jackson, B. V. Weber, D. Mosher, D. G. Phillips, S. J. Stephanakis, R. J. Commisso, N. Qi, B. H. Failor, and P. L. Coleman, Rev. Sci. Instrum. **79**, 10E717 (2008); R. D. McBride, T. A. Shelkovenko, S. A. Pikuz, D. A. Hammer, J. B. Greenly, B. R. Kusse, J. D. Douglass, P. F. Knapp, K. S. Bell, I. C. Blesener, and D. A. Chalenski, Phys. Plasmas **16**, 012706 (2009).
[17] P. F. Schmit, I. Y. Dodin, and N. J. Fisch, Phys. Plasmas **18**, 042103 (2011).
[18] S. A. Slutz, M. C. Herrmann, R. A. Vesey, A. B. Sefkow, D. B. Sinars, D. C. Rovang, K. J. Peterson, and M. E. Cuneo, Phys. Plasmas **17**, 056303 (2010).